Biology, Chemistry, and Environmental Sciences Faculty Articles and Research

Science and Technology Faculty Articles and Research

2007

Coupling Coherence Distinguishes Structure Sensitivity in Protein Electron Transfer

Tatiana Prytkova
Chapman University, prytkova@chapman.edu

Igor V. Kurnikov
Duke University

David Beratan
Duke University

Recommended Citation

Coupling Coherence Distinguishes Structure Sensitivity in Protein Electron Transfer

Coupling Coherence Distinguishes Structure Sensitivity in Protein Electron Transfer

Tatiana R. Prytkova, **Igor V. Kurnikov**[*], and **David N. Beratan**[†]
Departments of Chemistry and Biochemistry, Duke University, Durham, NC 27708, USA.

Abstract

Quantum mechanical analysis of electron tunneling in nine thermally fluctuating cytochrome b_{562} derivatives reveals two distinct protein-mediated coupling limits. A structure-insensitive regime arises for redox partners coupled through dynamically averaged multiple-coupling pathways (in seven of the nine derivatives) where heme-edge coupling leads to the multiple-pathway regime. A structure-dependent limit governs redox partners coupled through a dominant pathway (in two of the nine derivatives) where axial-ligand coupling generates the single-pathway limit and slower rates. This two-regime paradigm provides a unified description of electron transfer rates in 26 ruthenium-modified heme and blue-copper proteins, as well as in numerous photosynthetic proteins.

Many biological pathways depend on the facilitation of electron transfer (ET) processes by proteins (1–14). At the simplest level, this acceleration in rate can be explained by empirical models that omit the details of protein structure and describe the fact that proteins lower the barrier to electron tunneling by about 3 eV relative to that of vacuum tunneling (1, 14). However, ET rates can be slower or faster in different proteins, despite the electron's traveling a similar distance between donors and acceptors (R_{DA}) (1–3). These rate differences can arise because tunneling is faster through covalent bonds than through weak or nonbonded contacts (10), and the composition of the coupling medium between donor and acceptor varies with the primary, secondary, and tertiary structure of the protein (1, 2, 10).

The simplest model that accounts for such structural effects on ET rates is the pathway model (10), which identifies the most facile coupling routes between the donor and acceptor. Packing-density models analyze atom density between the donor and acceptor. The predictions of the pathway and packing-density models are nearly the same (4, 15). Nonetheless, there are many examples where an even simpler exponential model (14)

$$k_{ET} \propto \exp[-\beta R_{DA}] \quad (1)$$

, where k_{ET} is the ET rate and β is an exponential decay constant, can account for the observed ET rates without including three-dimensional details of protein structure.

[†]To whom correspondence should be addressed. david.beratan@duke.edu.
[*]Present address: Department of Environmental and Occupational Health, University of Pittsburgh, Pittsburgh, PA 15219–3130, USA.

The limits of validity for these simple tunneling models have been poorly understood, and understanding has been further hampered by the lack of sufficiently detailed data sets on ET rates for the same protein that would allow for meaningful comparisons; in comparing ET rates between different proteins, it is difficult to separate the electron-tunneling factors from the nuclear factors, or Marcus factors (16), that arise in the ET theory (1, 2). We have now analyzed a recent set of tunneling-limited ET rates obtained by Winkler and Gray for a Ru-modified heme protein [cytochrome (cyt) b_{562}]. The exponential distance-decay model accounts for some but not all of the observed rate dependences (17, 18). We provide an explanation for the different rate behaviors in this protein, which can also account for ET kinetic data in other Ru-modified heme proteins (including cyt c and myoglobin).

Here, we argue that some protein structures generate exponential decay of coupling with distance (as if the proteins were structureless tunneling barriers) by dynamically averaging multiple-coupling pathways. Other protein structures, in contrast, retain pathway-specific coupling characteristics that may be very different from the "average" protein coupling for that R_{DA} value. We explain why the protein-mediated coupling falls either in the pathway or average-barrier regime, and we also find that a simple metric—the coupling coherence parameter (19)—provides a reliable indicator of the coupling mechanism. We restrict our discussion to unimolecular ET between sites within a protein, although interprotein ET appears to be even more sensitive to structure than unimolecular ET (11, 12).

We briefly review the two structured-protein models (1, 10). The pathway model predicts

$$k_{ET} \propto \left\{ \prod_i \varepsilon_i^{bond} \prod_j \varepsilon_j^{bond} \exp[-\beta^{space}(r_j - r_0)/2] \right\}^2 \quad (2)$$

where Π represents a product, $\varepsilon^{bond} \sim 0.6$ and $\beta^{space} \sim 1$ Å^{-1} are decay parameters associated with the dominant-coupling route from donor to acceptor through a combination of bonded and nonbonded contacts, r_j is the length of each through-space contact, and r_0 is 1.4 Å. The pathway-based rate is well approximated by means of an atomic packing-density model (4, 15)

$$k_{ET} \propto \exp[-\beta^{space} f^{space} R_{DA}] \times \exp[-\beta^{bond}(1 - f^{space})R_{DA}] \quad (3)$$

where the β parameters describe tunneling decay through bond or space, and $1 - f^{space}$ is the fraction of space between the donor and acceptor that is filled with atoms (4). The pathway and packing-density rates (Eqs. 2 and 3) include explicit information about the protein fold that is not included in the simple exponential model (square-barrier tunneling model), which uses a single fitted β value. Fully quantum treatments sum together contributions to the tunneling rate that arise from the multiplicity of donor-acceptor (D-A) pathways that couple donor to acceptor (1, 2). In conformationally flexible systems, the mean square (ensemble-averaged) D-A coupling $\langle H_{DA}^2 \rangle$ determines the rate (20–22)

$$k_{ET} \propto \langle H_{DA}^2 \rangle \quad (4)$$

Here, we examine the tunneling-limited ET kinetics for Ru-modified cyt b_{562} (Fig. 1A) (18); each derivative explores the tunneling-mediation characteristics of a distinct protein region. All but two of these rates fit a simple square-barrier tunneling model (Fig. 1B). Two rates fall two orders of magnitude below the square-barrier (exponential distance-decay)model for tunneling in this protein. The ET kinetics in cyt b_{562} mirrors previous observations in Ru-

modified cyt c [one of eight tunneling-limited rates is two orders of magnitude below an exponential fit (17)] and in myoglobin [one of three tunneling-limited rates is orders of magnitude slower than expected based on distance analysis (17)]. Cyt c data appear in fig. S1.

We first used a previously developed ab initio Hartree-Fock method to compute ET rates in these cyt b_{562} systems (23, 24). The correlation between computed and observed ET rates appears in fig. S2. Except for the longest-distance derivative (His[86]), the measured and computed rates agree within a factor of four. This order of magnitude agreement, including a satisfactory description of the anomalously slow ET kinetics in the His[12] and His[73] derivatives, indicates that theory describes the essential aspects of ET kinetics in these complex systems. The computations include protein conformational averaging, solvation, and averaging of couplings over multiple ligand-field states with the use of methods described previously (23). The calculations explicitly include multiple-pathway interferences, without making empirical assumptions that are associated with dominant pathways or packing density.

We now examine the physical origin of the two slow ET rates, as well as the simple (exponential) distance dependence for the other seven derivatives. To perform this analysis, we computed D-A interactions for protein structure shapshots taken from classical molecular dynamics (MD) trajectories. Because the number of calculations needed for this analysis is large, we used an extended-Hückel Hamiltonian. Extended-Hückel analysis of D-A interactions in proteins has been used successfully in previous studies of Stuchebrukhov and Marcus (25), Kakitani (26), Onuchic (6), and others. Our analysis assumes metal-localized states to describe the $Fe^{2+} \rightarrow Ru^{3+}$ ET (17).

The string of computed coupling interactions allows us to calculate the Balabin-Onuchic coherence parameter, $C = \langle H_{DA} \rangle^2 / \langle H_{DA}^2 \rangle$ (19), for the ruthenated proteins. We expect C to be very small when numerous interfering coupling pathways contribute to the D-A interaction. In this limit, only average characteristics of the protein fold determine the ET rate. In contrast, when C is near unity, a dominant-coupling pathway mediates tunneling, and the observed rate is characteristic only of that pathway's structure. Indeed, the His[12] and His[73] derivatives of cyt b_{562} have C parameters of 0.6 and 0.5, respectively, whereas all other derivatives have C values of 0.1 or less (table S2).

Coupling values along 100-ps MD trajectories for His[12], His[70], and His[73] appear in Fig. 2. The coupling values along the MD trajectory for the His[73] ($C = 0.5$) and His[12] ($C = 0.6$) derivatives rarely change sign (Fig. 2, A and B), which is characteristic of the dominant pathway regime. The His[70] derivative [$C = 4 \times 10^{-3}$] has a coupling value that fluctuates about zero and a mean coupling value squared ($\langle H_{DA} \rangle^2$) that is orders of magnitude smaller than the mean squared coupling value ($\langle H_{DA}^2 \rangle$). This small C regime is characteristic of multiple interfering coupling pathways of comparable strength, so the $\langle H_{DA}^2 \rangle$ value is averaged over many pathways and is characteristic of the overall protein fold rather than of a single dominant-coupling pathway. In contrast, coupling in the large C regime is determined by the structure of the dominant-coupling pathway.

What aspects of structure in a single protein can generate this substantial difference in mechanism? Simple tunneling-pathway analysis of the cyt b_{562} His[12] and His[73] derivatives provides the answer. The two large C-parameter (dominant pathway) structures have coupling pathways linked to the heme through an axial ligand, but seven other derivatives each have surface Ru complexes that are coupled electronically by multiple pathways to the

heme edge. The tunneling-pathway analysis (fig. S3) reveals this aspect of protein connectivity.

Because of the large size of the heme-edge "target," coupling into the heme edge in cyt b_{562} generates multiple interfering pathways with mean squared values that reflect average coupling characteristics of the many pathways. The axial-ligand pathway derivatives, in contrast, have a smaller number of sizable coupling pathways leading to the heme (Fig. 3), because coupling routes must proceed through one single metal-ligand pathway bottleneck. In cyt b_{562}, this connectivity gives rise to single-pathway (large C value) mechanisms. Moveover, the axial ligand's van der Waals volume apparently serves to minimize the presence of multiple coupling routes to the prophyrin ring face. This contrasts with the large circumference heme-edge access provided by noncovalent interactions. In the case of cyt b_{562} (and for other Ru proteins, as described below), pure axial pathways have large C values (i.e., dominant pathways), are poorly "wired" to the heme, and produce slow tunneling-limited rates. It appears that dynamical averaging over many coupling pathways operates in cyt b_{562} for all heme-edge–coupled derivatives, producing simple (exponential) decay with distance as described by Eq. 1.

Is the observation of weak single-pathway (large C) axial coupling and strong multiple-pathway heme-edge coupling (small C) in cyt b_{562} relevant to other Ru-modified heme proteins and to native proteins? The one anomalously slow ET derivative in the Ru–cyt c family is the His[72] derivative (fig. S1) (17), and the dominant-coupling pathway to the heme is routed via an axial ligand. The anomalously slow His[83] derivative of the Ru-myoglobin family is also dominated by an axial-ligand pathway. All "average" rates in cyt c and myoglobin (i.e., those rates that fit well by a single exponential decay law) access multiple-coupling pathways, including heme-edge–coupled pathways. As such, our distinction between multiple-pathway heme-edge–coupling routes and axial-ligand–dominated single-coupling routes rationalizes all of the anomalously slow ET rate data among 20 ground-state Ru-modified heme proteins (3, 17).

Our heme-protein analysis indicates that exponential distance dependence for protein ET rates occurs in the small C multiple-pathway regime. Because small C values have been computed in nonheme proteins as well, we can further explore the correlation between small C values and exponential distance decay. Previous theoretical analysis of the blue-copper protein azurin indicates that all six Ru derivatives have very small C values (27), which is consistent with the measured single exponential decay of rates with distance in this protein for all derivatives (17). In azurin, the three strong coupling routes to the copper or the pathway cross-linking by hydrogen bonds provide likely physical sources of average-medium behavior. Although coherence parameter analysis remains to be performed for the Ru-modified high-potential iron protein (28), we expect that the anomalously slow Ru-His[50] derivative will also have a large C associated with a weak dominant-coupling pathway. Rates in all 26 ruthenated myoglobin, cyt c, cyt b_{562}, and azurin derivatives are explained within the dichotomy of an average-medium tunneling (small C) model or a single-pathway tunneling (large C) model. In Ru-modified heme proteins, heme-edge coupling produces average-medium behavior, whereas axial-ligand coupling generates pathway-specific D-A interactions.

Tunneling-limited ET rates in the photosynthetic reaction center (PRC) follow an exponential distance-decay law (4). Preliminary analysis of coherence parameters in the PRC charge transfer reactions indicates values of 10^{-2} or less, which are consistent with multiple edge-coupled pathways and average-medium behavior. We find similar behavior in the DNA repair protein photolyase, where ET couples two delocalized pi-electron states (29).

The accessibility of two coupling mechanisms seems essential for the analysis of evolutionary pressure on ET proteins. Earlier arguments regarding pathway evolution had been made along two lines. Simple (exponential) distance dependencies observed in the photosynthetic proteins led Moser, Dutton, and co-workers to suggest that evolution manipulates ET rates using R_{DA} and Marcus (nuclear) parameters (4). Gray, Winkler, and co-workers, in contrast, argued that strong pathways have evolved to accelerate ET in some proteins (5). Indeed, the structure of common biological redox cofactors seems to permit ET proteins to access both mediation regimes.

We suggest that, in the multiple-pathway regime, the evolutionary linkage between the specific protein fold and the ET rate is likely to be weak: In this regime, R_{DA} determines tunneling propensity. In the single-pathway large C regime, however, ET kinetics and protein structure are strongly linked. Although the Ru proteins only display slow rates in the dominant pathway regime, either strong or weak coupling pathways could arise in the dominant pathway regime, generating order of magnitude effects on the ET kinetics from protein structure. This structure-function perspective extends the pathway-evolution conjecture of Ramirez *et al.* (5), by accounting for the influence of thermal motion on the protein-mediated coupling, and also suggests that the Moser-Dutton (average-medium) view is valid in the multiple-pathway regime common to many large edge-coupled redox cofactors. Tunneling routes involving axial ligands seem to be the most likely candidates for kinetics that is sensitive to coupling pathway structure [e.g., the heme a to heme a_3 pathways in cyt c oxidase (5, 6)]. How often and where nature has used pathway-specific or multiple-pathway regimes remain to be determined by future analysis and experiments. Also, in the small C regime, proteins will have ET kinetics that are robust to modifications of single-pathway links (e.g., by manipulating hydrogen bonding), whereas pathway structural changes in the large C regime may have a larger influence on ET kinetics (30–32).

Supplementary Material

Refer to Web version on PubMed Central for supplementary material.

Acknowledgments

References and Notes

1. Skourtis SS, Beratan DN. Adv. Chem. Phys. 1999; 106:377.
2. Regan JJ, Onuchic JN. Adv. Chem. Phys. 1999; 107:497.
3. Gray HB, Winkler JR. Proc. Natl. Acad. Sci. U.S.A. 2005; 102:3534. [PubMed: 15738403]
4. Page CC, Moser CC, Chen X, Dutton PL. Nature. 1999; 402:47. [PubMed: 10573417]
5. Ramirez BE, Malmström BG, Winkler JR, Gray HB. Proc. Natl. Acad. Sci. U.S.A. 1995; 92:11949. [PubMed: 8618820]
6. Tan ML, Balabin IA, Onuchic JN. Biophys. J. 2004; 86:1813. [PubMed: 14990507]
7. Francisco WA, Wille G, Smith AJ, Merkler DJ, Klinman JP. J. Am. Chem. Soc. 2004; 126:13168. [PubMed: 15479039]
8. Stubbe J, Nocera DG, Yee CS, Chang MCY. Chem. Rev. 2003; 103:2167. [PubMed: 12797828]
9. Antony J, Medvedev DM, Stuchebrukhov AA. J. Am. Chem. Soc. 2000; 122:1057.
10. Beratan DN, Betts JN, Onuchic JN. Science. 1991; 252:1285. [PubMed: 1656523]
11. Hoffman BM, et al. Proc. Natl. Acad. Sci. U.S.A. 2005; 102:3564. [PubMed: 15738411]
12. McLendon G, Hake R. Chem. Rev. 1992; 92:481.
13. Kang SA, Crane BR. Proc. Natl. Acad. Sci. U.S.A. 2005; 102:15465. [PubMed: 16227441]

14. Hopfield JJ. Proc. Natl. Acad. Sci. U.S.A. 1974; 71:3640. [PubMed: 16592178]

15. Jones ML, Kurnikov IV, Beratan DN. J. Phys. Chem. B. 2002; 106:2002.

16. Marcus RA, Sutin N. Biochim. Biophys. Acta. 1985; 811:265.

17. Gray HB, Winkler JR. Q. Rev. Biophys. 2003; 36:341. [PubMed: 15029828]

18. Winkler JR, Di Bilio AJ, Farrow NA, Richards JH, Gray HB. Pure Appl. Chem. 1999; 71:1753.

19. Balabin IA, Onuchic JN. Science. 2000; 290:114. [PubMed: 11021791]

20. Daizadeh I, Medvedev ES, Stuchebrukhov AA. Proc. Natl. Acad. Sci. U.S.A. 1997; 94:3703. [PubMed: 9108041]

21. Troisi A, Nitzan A, Ratner MA. J. Chem. Phys. 2003; 119:5782.

22. Skourtis, SS.; Lin, J.; Beratan, DN. Modern Methods for Theoretical Physical Chemistry of Biopolymers. Starikov, EB.; Lewis, JP.; Tanaka, S., editors. New York: Elsevier; 2006.

23. Prytkova TR, Kurnikov IV, Beratan DN. J. Phys. Chem. B. 2005; 109:1618. [PubMed: 16851133]

24. This is one of a number of methods being developed with few adjustable parameters that may be used to compute coupling interactions in systems as complex as proteins. For related studies, see Barone V, Newton MD, Improta R. Chem. Phys. Chem. 2006; 7:1211. [PubMed: 16680796] andKawatsu T, Kakitani T, Yamato T. J. Phys. Chem. B. 2002; 106:11356.

25. Stuchebrukhov AA, Marcus RA. J. Phys. Chem. 1995; 99:7581.

26. Nishioka H, Kimura A, Yamato T, Kawatsu T, Kakitani T. J. Phys. Chem. B. 2005; 109:1978. [PubMed: 16851182]

27. Skourtis SS, Balabin IA, Kawatsu T, Beratan DN. Proc. Natl. Acad. Sci. U.S.A. 2005; 102:3552. [PubMed: 15738409]

28. Babini E, et al. J. Am. Chem. Soc. 2000; 122:4532.

29. Prytkova TR, Beratan DN, Skourtis SS. Proc. Natl. Acad. Sci. U.S.A. 2007; 104:802. [PubMed: 17209014]

30. Zheng YJ, Case MA, Wishart JF, McLendon GL. J. Phys. Chem. B. 2003; 107:7288.

31. van Amsterdam IMC, et al. Nat. Struct. Biol. 2002; 9:48. [PubMed: 11740504]

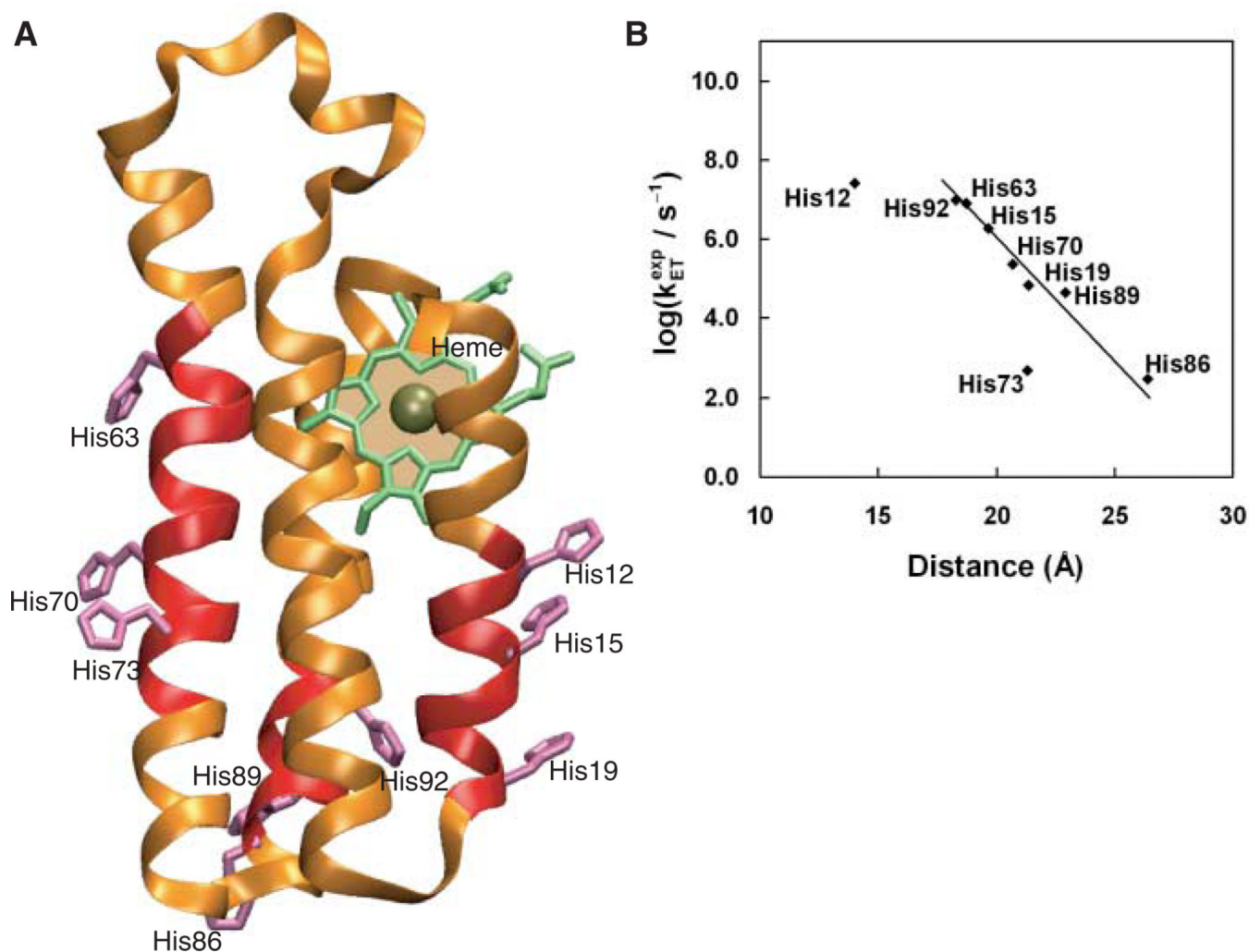32. Lin J, Balabin IA, Beratan DN. Science. 2005; 310:1311. [PubMed: 16311331]

Fig. 1.
(**A**) Ribbon diagram indicating the positions of the nine Ru-modified His sites on cyt b_{562}.
(**B**) Experimentally measured tunneling-limited ET rates for each of these nine cyt b_{562} derivatives (18). The His[12] and His[73] derivatives have anomalously slow rates that fall well below an average exponential (square-barrier tunneling) model, which are fit here with a decay constant of 1.3 Å^{-1}.
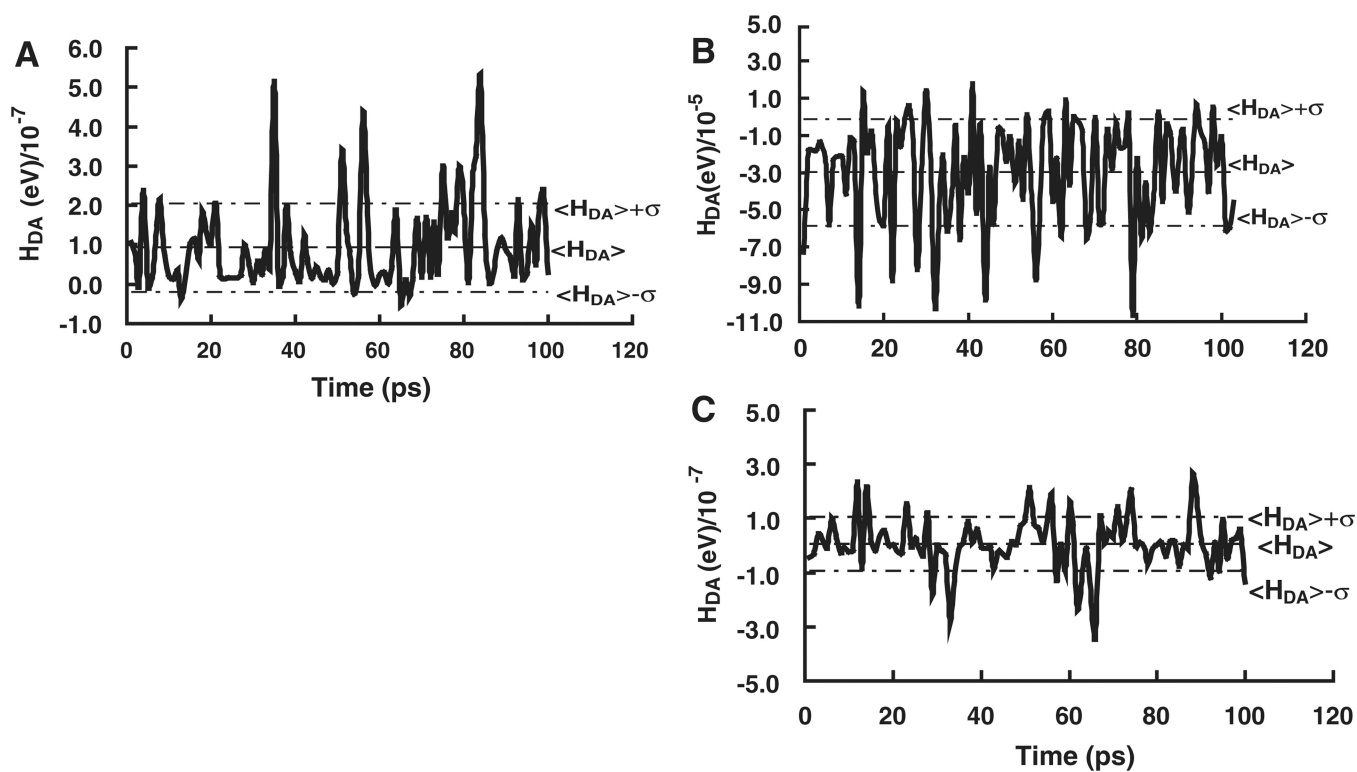
Fig. 2.
Electronic couplings versus time. (**A**) His[73] ($C = 0.5$), dominant-coupling pathway regime; (**B**) His[12] ($C = 0.6$), dominant-coupling pathway regime; (**C**) His[70] ($C=4\times10^{-3}$), multiple-pathway mechanism. Note the frequent sign flips in (C), which are consistent with a multiple-pathway mechanism. In (A) and (B), $\langle H_{DA} \rangle^2$ differs by only about a factor of two from $\langle H_{DA}^2 \rangle$. Geometry snapshots were captured each 1 ps and input to the extended-Hückel coupling calculations.
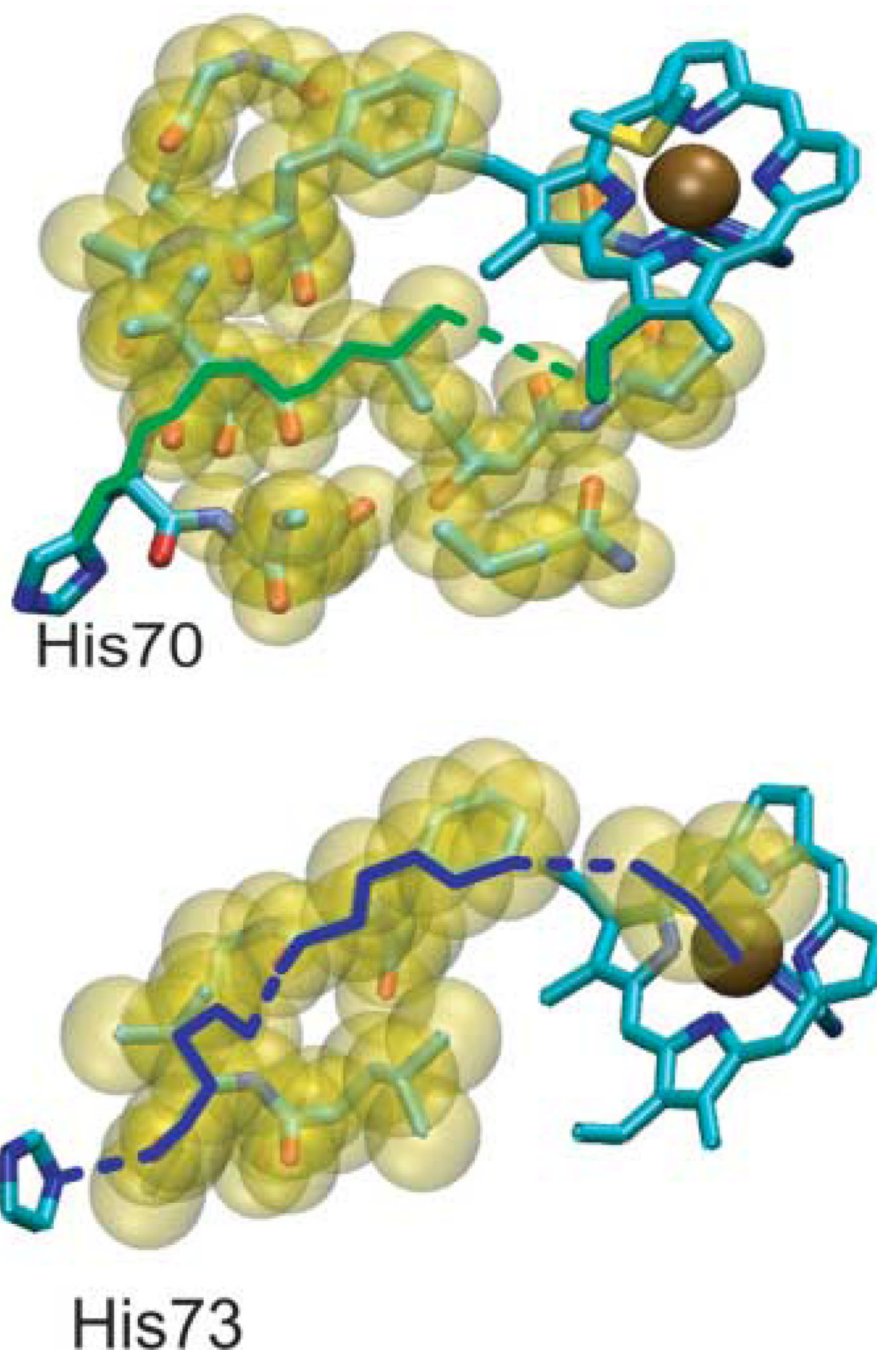
Fig. 3.
Pruned protein media [5% cutoff criterion (23)] for His[70] (average-medium or multiple-pathway regime, small C parameter) and His[73] (single-pathway regime, large C parameter). Both proteins have ET distances of ~20 Å metal-to-metal. The strongest single pathways are noted with solid and dashed lines. Spheres are shown on atoms included in the quantum tunneling analysis (23).